Organic & Biomolecular Chemistry

RSC Publishing

PERSPECTIVE

View Article Online
View Journal | View Issue

Supramolecular chemical biology; bioactive synthetic self-assemblies

Cite this: *Org. Biomol. Chem.*, 2013, **11**, 219

Katja Petkau-Milroy and Luc Brunsveld*

The regulation of recognition events in nature *via* dynamic and reversible self-assembly of building blocks has inspired the emergence of supramolecular architectures with similar biological activity. Synthetic molecules of diverse geometries self-assemble in water to target biological systems for applications ranging from imaging and diagnostics, through to drug delivery and tissue engineering. Many of these applications require the ability of the supramolecular system to actively recognize specific cell surface receptors. This molecular recognition is typically achieved with ligands, such as small molecules, peptides, and proteins, which are introduced either prior to or post self-assembly. Advantages of the non-covalent organization of ligands include the responsive nature of the self-assembled structures, the ease of supramolecular synthesis and the possibility to incorporate a multiple array of different ligands through premixing of the building blocks. This review aims to highlight the diversity of self-assembled nanostructures constructed from mono-disperse synthetic building blocks; with a particular focus on their design, self-assembly, functionalization with bioactive ligands and effects thereof on the self-assembly, and possible applications.

Received 12th September 2012,
Accepted 29th October 2012

DOI: 10.1039/c2ob26790j

www.rsc.org/obc

1. Inspired by nature

Nature is composed of vast arrays of well-ordered functional nanostructures, which result from the self-assembly of disordered biomolecular units.[1] Examples include the self-assembly of proteins and RNA to form the ribosome – the translationary machinery of the cell – as well as the rapid assembly and

Laboratory of Chemical Biology, Department of Biomedical Engineering, Eindhoven University of Technology, Den Dolech 2, 5612AZ Eindhoven, The Netherlands. E-mail: l.brunsveld@tue.nl; Fax: +31 40 2478367; Tel: +31 40 2472870

Katja Petkau-Milroy

Katja Petkau-Milroy (1982) studied chemistry at the Technische Universität Dortmund, where, after stays at the Universidad Complutense de Madrid and the Max Planck Institute of Molecular Physiology, she graduated in 2008. In 2012 she received her PhD in chemical biology at the Eindhoven University of Technology under the supervision of Prof. L. Brunsveld. Her PhD research focused on the synthesis and biological evaluation of multivalent supramolecular polymers as platforms for protein assembly and cell surface recognition. She is currently working as a postdoctoral researcher in Eindhoven on the development of nanoparticles for biosensing and imaging.

Luc Brunsveld

Luc Brunsveld (1975) is professor of chemical biology at the biomedical engineering department of the Eindhoven University of Technology. After obtaining a PhD in supramolecular chemistry with E.W. Meijer he was a Humboldt Fellow at the Max Planck Institute of Molecular Physiology with H. Waldmann and medicinal chemistry group leader at Organon. In 2005 he started as group leader at the CGC in Dortmund and subsequently moved to Eindhoven in 2008. His interests are in protein-protein interactions with a specific focus on nuclear receptors and in combining supramolecular chemistry with chemical biology.

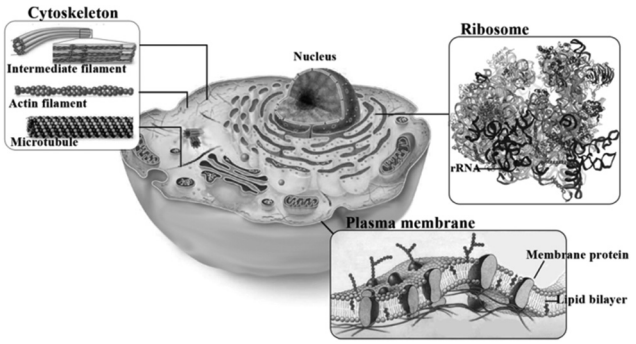

Fig. 1 Eukaryotic cell; insets: cytoskeleton with three major cytoplasmic supramolecular polymers – microtubules, intermediate filaments, and actin filaments;[2] plasma membrane with transmembrane proteins; crystal structure of a eukaryotic ribosome,[3] a highly complex assembly of more than 50 protein subunits and several RNAs (black).

disassembly of actin and microtubule filaments and the self-assembly of phospholipids to form cell membranes (Fig. 1). The most significant advantage of such non-covalent self-assemblies is the generation of adaptable and dynamic nano-sized structures.

Nature frequently uses self-assembly to orchestrate recognition events. This is especially the case for the cell membrane: a highly selectively permeable barrier consisting of a lipid bilayer with integral proteins which is essential for cell survival and function. The non-covalent self-assembly of transmembrane proteins in the plasma membrane enables dynamic movement and the spontaneous clustering of receptors: a crucial requirement for the function of growth factor-mediated cell signaling,[4] integrin-mediated cell adhesion[5] and T-cell activation,[6] to name but a few. The phospholipids are asymmetrically dispersed between the outer and the inner leaflet of the lipid bilayer, and this asymmetric disequilibrial distribution is maintained by energy dependent lipid transporters. The anionic phospholipid, phosphatidylserine (PS), is *via* this process normally restricted to the inner leaflet. However, in dying and activated cells, specific localization is no longer maintained, resulting in the translocation of PS to the outer leaflet;[7] a process only possible through the non-covalent rearrangement of lipid assembly in the plasma membrane. In nature, this phenomenon triggers the uptake and removal of early apoptotic cells by macrophages bearing PS recognizing receptors. In biochemistry, PS binding probes, for example liposomes displaying several annexin V proteins,[8] are now widely used as markers of early apoptotic cells.

The three major cytoplasmic supramolecular polymers – microtubules, intermediate filaments, and actin filaments – spontaneously assemble from short monomers into long uniform structures. The polymerization process is spatio-temporally regulated in response to external stimuli. Microtubules, cytoplasmic tubular fibres, which self-assemble from alternating protein subunits (Fig. 1), are involved in many cellular functions such as intracellular transport and chromosome segregation during cell division. Cell motility is regulated by the rapid assembly of filamentous actin.[9] The dynamic function of these processes is intrinsically coupled to the capacity of actin and microtubules to rapidly polymerize and depolymerize,[10] a requirement which can only be met with the help of dynamic supramolecular assembled systems.

The self-assembly of these biomolecules is a consequence of specific, local and non-covalent interactions, which include hydrogen bonding as well as electrostatic and hydrophobic interactions. Since the intrinsic nature of self-assembly is a 'bottom-up' construction of higher-order structure from monomeric building blocks, the final assembly is stabilized by many, relatively weak, non-covalent interactions distributed over the whole molecular volume. This intrinsic nature offers an excellent platform for the construction of multivalent ligands, which can simultaneously interact with multiple complementary receptors. Such multivalent interactions are essential for multiple biological recognition events since increasing the number of existing interactions or combining diverse molecular interactions leads to high-affinity molecular recognition without the need to evolve stronger and more complex binders.[11,12]

Nature has created a diverse range of structures and functions at the cellular and sub-cellular level using non-covalent self-assembly, which has inspired the emergence of supramolecular chemistry. Supramolecular chemistry studies the non-covalent interactions in and between molecules, and the resulting multimolecular complexes.[13,14] Starting with small synthetic supramolecular systems derived from simple building blocks,[15] an increased understanding of intermolecular interactions has led to the supramolecular synthesis of multimolecular architectures with a vast array of shapes, compositions and functionalities and with numerous applications in the field of materials science.[16] In most of these cases, however, and in contrast to nature, these supramolecular materials have been self-assembled in the solid or gel state or in organic solvents. The development of supramolecular architectures filled with the capacity to assemble under dilute conditions in water or buffered media[17–20] has since opened up the field of supramolecular chemistry to supramolecular chemical biology, where supramolecular chemistry is applied to the study of biological processes.[21]

2. Supramolecular chemical biology

2.1 Arising applications of self-assembling materials

Synthetic supramolecular architectures in water could find diverse applications, ranging from imaging to diagnostics, and from drug delivery to tissue engineering. Advantages of the non-covalent organization of ligands compared to the organization of ligands in a covalent fashion on polymeric scaffolds include the responsive nature of the self-assembly process, the ease of supramolecular synthesis and the possibility to incorporate a multiple array of different ligands through intermixing of building blocks. Since the development of

supramolecular chemical biology, several applications for self-assembling nanostructures have been brought forward.

Many of the undesired side-effects of small drug molecules arise, amongst others, from the fact that they are non-specifically taken up by healthy cells. Typically, only a small percentage of the drug actually reaches the target or tissue of interest. The selective treatment of diseases with minimal side-effects, the so-called "magic-bullet" which was proposed by Paul Ehrlich in 1901,[22] is nowadays still under development. To improve drug efficacy and safety, it has proved desirable to encapsulate drugs so as to target them to a specific site of disease.[23] In this case, the drug carrier should allow gradual, or even triggered, release of the drug and be biodegradable. A certain size of approximately 100 nm is beneficial for long circulation times in the body in order to increase drug accumulation at the site of interest. Self-assembling systems of the vesicular sort might combine many of the desired properties of the drug encapsulation strategy with the ability to be functionalized with (several) targeting ligands. Together with liposomes, viral capsids and polymerosomes are promising candidates in this growing research area.[24–26]

The goal of targeted imaging in diagnostics is to achieve a significant enhancement of contrast at the targeted site in a non-invasive manner. Actively targeted imaging requires the attachment of targeting ligands and imaging probes (fluorophore, contrast agent) to the same molecular entity. The incorporation of several imaging probes, which should be facilitated in self-assembling structures, allows for multimodal imaging: the combination of several imaging techniques to synergistically improve resolution and sensitivity.[27] Additionally, self-assembling contrast agents might combine the benefits of both high and low molecular weight contrast agents, *i.e.* high relaxivity and the complete excretion from the body over time due to disassembly into monomers on dilution.

In tissue engineering, self-assembling biomaterials are promising candidates for the construction of cell-interactive (3D) matrices.[28–33] In particular, peptide-based self-assembling materials that are capable of forming hydrogels are used to generate adaptable cell-culture matrices.[34] The modular self-assembly of proteins, peptides and peptide derivatives into hydrogels enables the independent, simultaneous and systematic tuning of several properties, leading to optimized cell–matrix interactions in cell culture and for regenerative medicine.[35] In contrast, for covalent polymer networks, this optimization of cell–matrix interactions has proved to be more difficult. Recently, it was as well shown that the presentation of intermixed binding epitopes led to improved cell adhesion when compared against gels with separately assembled binding epitopes.[36] The density and distribution of adhesive ligands within a substrate can influence integrin clustering and with it cell adhesion, migration and phenotype (Fig. 2).[37]

Apart from the potential biomedical applications of supramolecular biomaterials, the detailed investigation of their self-assembly, especially of *de novo* designed building blocks, helps with the understanding of how to predict and control the shape and size of self-assembled nanostructures, which remains an imposing challenge in the field of supramolecular chemistry.

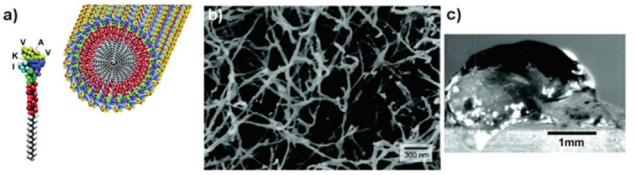

Fig. 2 Self-assembly of peptide amphiphiles for regenerative medicine. (a) Illustration of an IKVAV-containing peptide amphiphile and its self-assembly into nanofibres. (b) Scanning electron micrograph of an IKVAV nanofibre network formed by addition of cell media. (c) Micrograph of an IKVAV nanofibre gel surgically extracted from an enucleated rat eye after intraocular injection of the peptide amphiphile solution. Adapted from ref. 37 with permission from American Association for the Advancement of Science.

2.2 Ligand functionalization of self-assembling materials

Many of the above sketched applications require the supramolecular systems to be capable of actively targeting specific cell surface receptors. Targeting is typically achieved through functionalization of the materials under study with ligands, such as small molecules, peptides, proteins and antibodies. As mentioned above, the intrinsic nature of self-assembled systems – the construction of higher-order structure from monomeric building blocks – could be exploited to facilitate multivalent ligand display.[38] The ligands can either already be part of the monomeric supramolecular building blocks (pre-functionalization) or introduced post self-assembly *via* (non) covalent attachment to appending reactive groups (post-functionalization).

Combining the bioactive and the self-assembling epitope in one building block, the so-called pre-functionalization approach, enables the generation of nanomaterials with controlled ligand display (Fig. 3). The ligand density can be tuned through intermixing of building blocks featuring different ligands or those lacking any bioactive epitope.[39–41] A limitation of the pre-functionalization strategy is the need for the bioactive ligands to be compatible with the synthetic preparation of the building block and with the supramolecular synthesis, *i.e.* the self-assembly process of the final supramolecular architecture. The introduced ligand should not hinder the self-assembly. Typically, ligands such as carbohydrates, peptides and aptamers are suitable for the pre-functionalization strategy, because of their robust molecular structures, whereas more environment sensitive ligands such as larger, folded proteins might require an alternative functionalization approach.

The addition of functional epitopes to the bare supramolecular scaffolds post self-assembly would alternatively permit the introduction of a wide range of ligands using both synthetic and enzymatic approaches.[42–45] The non-decorated supramolecular scaffold acts as a versatile platform that can enable rapid functionalization in the aqueous environment in which it is formed. This post-functionalization approach would provide rapid access to diverse applications after

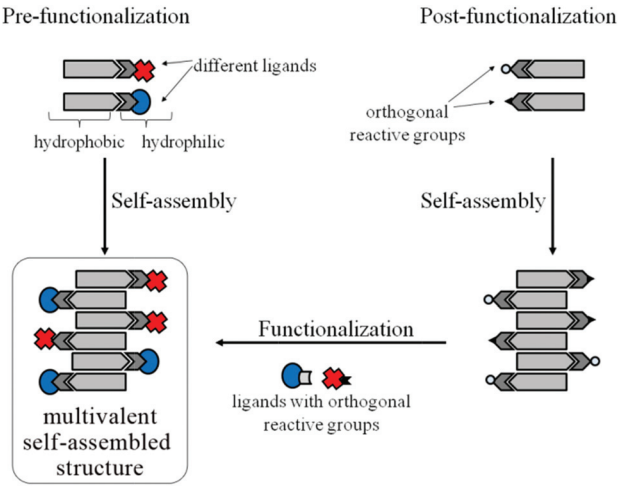

Fig. 3 Pre- and post-functionalization of self-assembling materials. Using the pre-functionalization approach, heterovalent structures are generated *via* co-assembly of differently functionalized building blocks. To generate heterovalent structures *via* post-functionalization the incorporation of several orthogonal reactive groups is required, which can be functionalized with a ligand after the self-assembly.

functionalization of the supramolecular scaffold without the need for redesign and *de novo* synthesis. The precise control over the introduced ligand density, however, might be limited to, for example, the reactivity and accessibility differences on different sites of the scaffold. Orthogonal functional groups could be introduced into the supramolecular building block of the bare self-assembled scaffold to enable the attachment of different functionalities *via* post-functionalization. The wide array of reactions that can be applied for post-functionalization in aqueous solution, such as NHS-, maleimide-coupling, azide–alkyne cycloaddition, Staudinger ligation and the suicide-enzymes such as SNAP-tag have recently been reviewed elsewhere.[43,44,46]

The main focus of this review will be to highlight the broad diversity of self-assembled nanostructures in water, built-up from mono-disperse non-polymeric synthetic building blocks; in particular emphasizing their design, self-assembly, functionalization with bioactive ligands and possible applications, which will be illustrated in the case of a few examples. Specific focus will be on the molecular interplay of the self-assembling, structuring element with the bioactive element. Polymer and block copolymer assemblies (polymersomes),[47,48] virus assemblies,[49] DNA assemblies[50] as well as non self-assembling nanoparticles[51] are other promising scaffolds used in imaging, targeting and drug delivery applications, which are not dealt with here.

3. Self-assembling bioactive nanostructures

The phase separation between hydrophobic and hydrophilic parts of an amphiphilic molecule in water plays an essential role in living systems (*e.g.* for the formation of membranes and for protein folding) and is now widely used as a powerful approach to form complex nano-architectures. In aqueous solution, amphiphilic molecules aggregate into micelles if their concentration lies above the critical aggregation concentration (CAC). For natural phospholipids, the CAC is approximately 10^{-8} mol L^{-1}.[52] The architectures formed by linear amphiphiles might be spherical, cylindrical or plate-shaped and the shape depends on factors such as temperature, concentration and the structure of the amphiphile itself; *i.e.* the hydrophobic–hydrophilic balance and the geometry of the amphiphile.[53]

3.1 Liposomes

Liposomes were initially used as model systems to mimic biological membranes.[54] These small self-assembled spherically shaped lipid vesicles are produced from natural non-toxic phospholipids and cholesterol with the lipid bilayer encapsulating an aqueous compartment. Liposomes can be easily varied in terms of their composition (*e.g.* using mixtures of chemically modified lipids), size and their ability to encapsulate different ligands, resulting in a large number of applications in drug delivery[55] and targeted imaging with broad applications and interest in industry and academia.[53]

A prerequisite for the aforementioned applications is the functionalization of liposomes with targeting ligands. The typical preparation method of liposomes involves the evaporation of an organic solvent, rehydration, followed by sonication and extrusion, which tends to limit the types of ligands that can be introduced prior to assembly. This limitation can be successfully circumvented through the introduction of functional reactive groups – using, for example, synthetically modified lipids or cholesterol – and post-assembly ligand decoration (Fig. 4).[56] Liposomes exposing several types of cell recognition ligands, from small molecules such as folic acid to large proteins including antibodies, have been generated and studied.[57] The decoration of liposomes with polyethylene glycol (PEG) has helped to elongate *in vivo* circulation times from a few minutes to several hours and prevent accumulation in the liver and spleen.[58] In a recent example by Kluza *et al.* it was shown that simultaneous targeting of two different receptors ($\alpha_v\beta_3$ integrin and galectin-1), so-called dual-targeting,

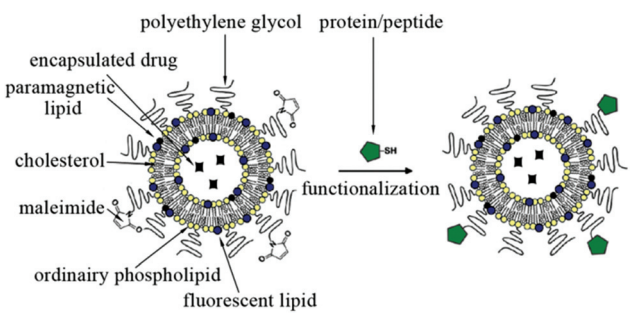

Fig. 4 Functionalized drug-encapsulating liposomes. Adapted from ref. 56 with permission from American Chemical Society.

synergistically improves liposomal uptake.[59] Simultaneous targeting was achieved *via* post-functionalization with two different types of ligands. Incorporation of fluorescent and paramagnetic lipids enabled evaluation and imaging using different techniques. The strong antiproliferative activity of these liposomes shows the potential of theranostics: a combination of diagnostics with therapy.[55] Additionally, liposomes not only allow for the inclusion of drugs and imaging agents, but as well nanocrystals such as iron oxide nanoparticles, gold nanoparticles and quantum dots, thus enabling the chemical surface functionalization of these nanocrystals.[55,56]

All these insights into self-assembly of natural phospholipids into liposomes have helped to develop different types of fully synthetic amphiphiles to generate a wide range of nanostructures as will be illustrated in the following sections.

3.2 Peptidic building blocks

Protein folding and with it protein function is encoded by the specific order of the 20 natural amino acids in the peptide sequence. While based on only a limited set of monomers, an almost unlimited structural diversity can be achieved through sequence adaptations. Besides the extensive use of peptide sequences to mimic the functional domains of large proteins, the ability to program a vast array of structures through changes in sequence *via* straightforward solid-phase synthesis has led to the use of peptides as self-assembling building blocks. In particular, the combination of bioactive and self-assembling epitopes generates customized nanomaterials for various biomedical applications.[60,61] Inter- or intramolecular hydrogen bonding between the carbonyl group and amine protons of the amide bond, which is a proton acceptor and donor in one, and the electrostatic and hydrophobic interactions of side-chains are responsible for protein folding, leading to differently structured and unstructured protein-folding (secondary) motifs. The most common structured motifs used are alpha-helices and beta-sheets.

3.2.1 Beta-sheet based self-assembly. Self-assembling beta-sheet structures, also referred to as amyloid-like structures, are mostly designed through alternating placement of positively charged, hydrophobic and negatively charged amino acids.[42] Electrostatic interactions between oppositely charged amino acid side-chains and solvophobic effects between hydrophobic side chains drive the proper interchain backbone hydrogen bonding.[62] The ability of these beta-sheets to pair *via* edge-to-edge and face-to-face packing leads to the formation of beta-sheet ribbons and tapes, which can bundle through lateral interactions into thicker fibres (Fig. 5a).[63] Through sophisticated design, up to four different peptides were shown to co-assemble into one fibril,[64] indicating the possibility to incorporate diverse functionalities through co-assembly.

The beta-sheet based self-assembled materials can exist with one or both of their N- or C-termini free, which allows for ligand functionalization. Besides the introduction of proteins through recombinant protein–peptide fusions,[65,66] the building blocks for beta-sheet fibrils were decorated with peptides,[67–69] biotin[70] and carbohydrates[71,72] prior to self-assembly.[42,73] The introduction of hydrophilic ligands at the N- or C-termini, however, can influence the self-assembly process, as shown for the functionalization with polyethylene glycol (PEG) groups.[71,72]

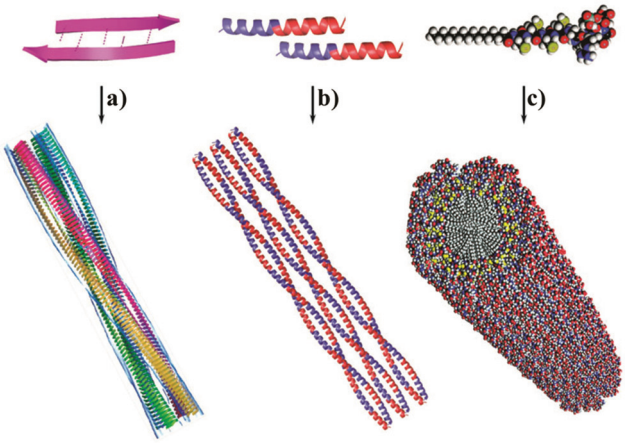

Fig. 5 Types of peptide-based self-assemblies; (a) beta-sheet based self-assembly, (b) alpha-helix based self-assembly, (c) peptide amphiphile based self-assembly. Adapted from ref. 42 with permission from the Royal Society of Chemistry.

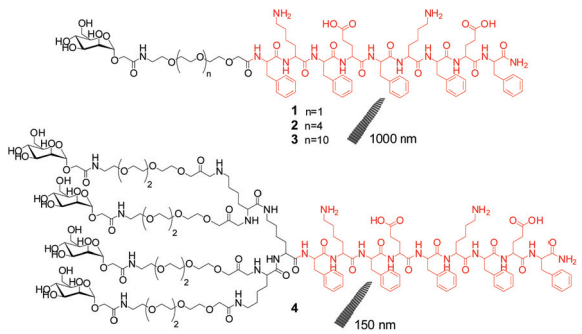

Fig. 6 Nanoribbons formed by mannose functionalized beta-sheet based amphiphiles.[71,72]

To illustrate, Lim *et al.* have synthesized amphiphiles consisting of a beta-sheet forming peptide (FKFEFKFE) and either linear or dendritic mannose functionalized PEG chains (Fig. 6). The dendritic PEG chains interfered with the self-assembly process, leading to the premature termination of fibrils.[71] Decoration with linear PEG chains induced a stronger association of the beta-sheet bilayer and more stable fibres. When testing for inhibition of bacterial motility (*E. coli*), similar inhibition was observed for all fibrils. However, the formation of bacterial clusters by interconnecting the pili of different bacteria was only induced by the long nanoribbons formed by **1**, **2** and **3**. The inhibition of bacterial motility could additionally be fine-tuned through co-assembly of **3** with the same building-block displaying non-binding glucose.[72]

3.2.2 Alpha-helical self-assembly. A key building-block of natural proteins, the alpha-helix, is a right-handed helix which is stabilized by intramolecular backbone hydrogen bonding between the carbonyl group (i) and the amide hydrogen four

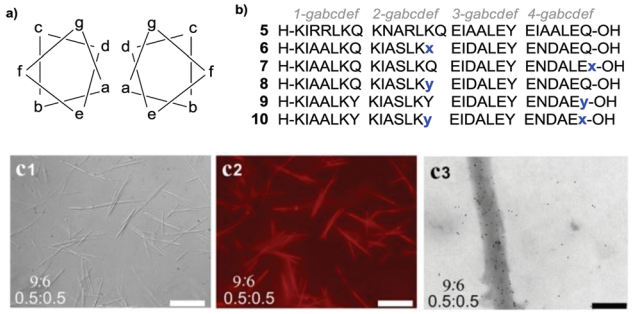

Fig. 7 Alpha-helical self-assembly. (a) Helical wheel diagram. (b) Peptide sequences used by the group of Woolfson[77] for self-assembly; y = lysine ε-azide, x = allylglycine. (c) DIC (c1, scale 10 μm), fluorescence microscopy (c2, scale 10 μm) and TEM (c3, scale 200 nm) images of dual-functionalized self-assembling fibers. **6** and **9** were mixed in a 1 : 1 ratio and subsequently functionalized with a biotinylated thiol-containing peptide and with rhodamine alkyne. To visualize the functionalization with the biotinylated peptide, the fibres were incubated with streptavidin-nanogold prior to TEM studies. Adapted from ref. 77 with permission from Elsevier.

residues further along the chain (i+4). Alpha-helices have 3.6 residues per turn, which align each third residue on top of each other (Fig. 7a). Introducing a pattern of polar and hydrophobic amino acids three residues apart generates an amphiphilic helix. The hydrophobic faces of several amphiphilic helices (residues a and d) can wrap around one another forming a so-called coiled-coil with the polar faces (residues b, c and f) exposed to the environment.[74] In accordance with the well-established sequence-to-structure rules, three to five heptad repeats of HPPHPP, with H being a hydrophobic and P a polar amino acid, are required to form stable structures.[75] For assembly into long and thick fibrils, the amphiphilic alpha-helices are designed with 'overhangs', which facilitate end-to-end assembly (Fig. 5b).[76]

The pre-functionalization of coiled-coil based self-assembling peptide fibres, developed by the group of Woolfson, *via* the intermixing of bare and ligand bearing peptides showed only poor incorporation of the ligand bearing peptide (~0.5% of the total peptide).[78,79] The alpha-helical peptides form crystalline-like assemblies, which are disfavoured on introduction of "molecular defects" such as small molecule ligands. For the incorporation of ligands, the same research group then applied the post-functionalization approach. Modified amino acids carrying azide and alkene moieties were introduced at the f position, furthest away from the coiled-coil interface (Fig. 7). This led in most cases to the formation of alpha-helical fibres. Using copper-catalyzed azide–alkyne cycloaddition and the photoinitiated thiol–ene reaction, the self-assembled fibres were decorated with different ligands and dual-functionalization of fibres assembled from mixtures of **6** and **9** with biotin and a dye was successfully achieved (Fig. 7c), thus forming a basis for further applications.[77]

The incorporation of an RGD sequence into longer alpha-helical coiled-coil peptides by Villard *et al.* reduced the size of the formed oligomers from around 80 to 5 self-assembling monomers, highlighting the sensitivity of the alpha-helical based system to structural changes. Once immobilized on a substrate, these short RGD-displaying self-assembling peptides were capable of promoting integrin αVβ3-dependent cell adhesion.[80]

3.2.3 Peptide amphiphiles. Over the last decade Stupp and co-workers have developed a class of amphiphilic molecules, the so-called peptide amphiphiles (PAs), which self-assemble into cylindrical micelles in dilute aqueous solutions (Fig. 5c).[81,82] The PAs consist of an alkyl chain linked to a peptide segment. The peptide segment itself features a structuring element followed by a charged amino acid and finally the bioactive epitope. The structuring peptide segment is composed of a β-sheet forming hydrophobic amino acids. Through intermolecular hydrogen bonding the peptide segment stabilizes and dictates the final shape of the self-assembly, as the lipid tail alone favours the formation of spherical and not cylindrical micelles. Furthermore, the charged amino acid provides enhanced solubility in water, while repulsive charge–charge interactions prevent the amphiphiles from assembling, unless the charge is shielded through adjustment of pH or salt concentration. This has enabled applications in regenerative medicine, as unassembled PAs can be combined with for example growth factors and cells. Upon injection into tissue, the charges of the PAs are neutralized by electrolytes and the PAs form a gel network encapsulating the desired payload.[83]

Incorporation of the neurite-promoting laminin-derived epitope IKVAV (**11**, Fig. 8a) at high densities on the surface of the assembled nanostructures induced rapid and selective differentiation of neural progenitor cells into neurons. The selective differentiation was even greater when compared to cells cultured with laminin, presumably due to higher epitope densities (Fig. 2).[37] *In vivo*, when injected into a mouse spinal cord injury model, the regeneration of the injury was facilitated.[83]

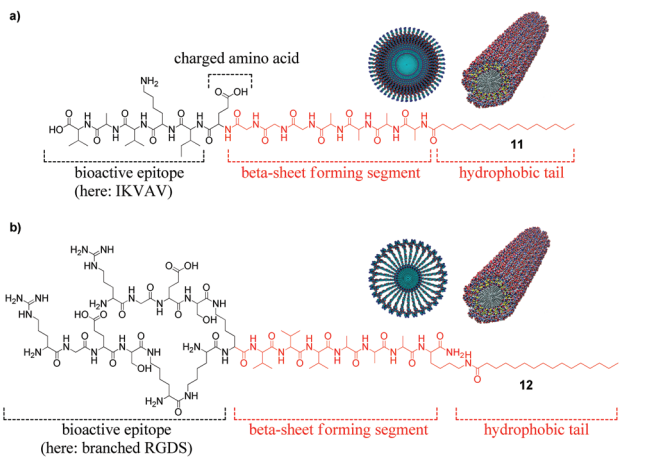

Fig. 8 Self-assembling peptide amphiphiles (PA). (a) Salt and pH sensitive PA **11** bearing an IKVAV peptide motif and cross-section through the cylindrical micelle formed; (b) Branched PA **12** with two linear RGDS sequences as bioactive epitope and cross-section through the cylindrical micelle formed. The micelle cross-sections were adapted from ref. 84 with permission from Elsevier.

Displaying the cell-adhesion epitope RGDS, the artificial PA matrix enhanced cell adhesion and receptor clustering compared to fibronectin. Signal accessibility was varied through changes in molecular architecture by utilizing (double-) branched PAs (**12**, Fig. 8b). The self-assembled structure was not changed, underlining the stability of the design, allowing incorporation of different types of peptide sequences. The lower packing densities of branched PAs (see micelle cross-section Fig. 8) led to increased epitope motion, improving cell adhesion, spreading and migration. A lower packing density of linear PAs could as well be achieved, through mixing with a PA lacking the bioactive epitope.[84]

Both examples show that the high density display of the hydrophilic bioactive epitope on the surface of the assembled nanostructure outperforms protein containing matrices. At the same time, the supramolecular assembly of these PAs allows tunability of ligand density either through changes in design or *via* simple intermixing of different peptide amphiphiles. A detailed overview of numerous further applications of PAs, for example in drug encapsulation, magnetic resonance imaging, mineralization, surface patterning and angiogenesis, can be found in *e.g.* ref. 85 and 86.

3.3 Self-assembly driven by non-peptidic units

The synthetic accessibility to novel and diverse non-peptidic linear amphiphilic structures has greatly expanded the scope of shapes, sizes and stabilities achievable for self-assembled structures. In the following section this will be illustrated using three selected examples.

Combining the features of lipids with the functions of bioactive peptides, amongst others, the group of Lee has investigated the influence of lipid composition on the stability and morphology of peptide–lipid conjugates. As an example, a cell-penetrating peptide, Tat, was coupled to hydrophobic branched lipids. Functionalized with a single stearic acid, **13** did not self-assemble in water. Two stearic acids were required for the assembly into spherical micelles (**14**) and cylindrical micelles were observed using the tetrameric lipid (**15**). Changing from dimeric to tetrameric lipid as well lowered the CAC almost 10-fold, from 208 μM for **14** to 21 μM for **15** (Fig. 9). The encapsulated dye Nile Red was efficiently delivered into the cytoplasm of HeLa cells.[87] The same group has as well self-assembled Tat using a short beta-sheet forming peptide, instead of a lipid tail. In contrast to the absence of self-assembly using one stearic acid, self-assembly at low concentrations was observed using a short beta-sheet forming peptide as the self-assembling unit.[67] The self-assembly of Stupp's peptide amphiphiles, containing a beta-sheet forming segment next to a lipid tail, resulted in stable cylindrical micelles irrespective of the (branched) peptide sequence,[84] highlighting the higher stability of beta-sheet based self-assembly. On the other hand, a larger diversity in adaptive morphology can be obtained using lipid-based systems.

To study multivalent carbohydrate-mediated interactions the group of Lee has developed a library of self-assembled nanostructures based on mannose functionalized aromatic

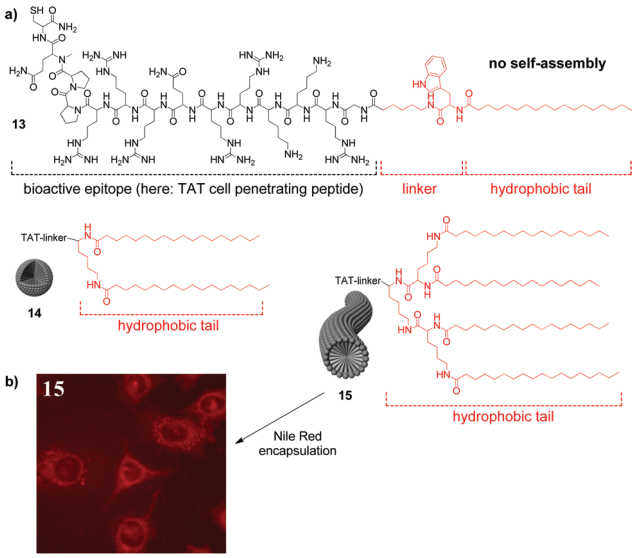

Fig. 9 Lipid based self-assembly of the cell-penetrating peptide Tat. (a) Functionalization of Tat with a single stearic acid (**13**) did not lead to self-assembly. Two stearic acids (**14**) led to the formation of spherical micelles, whereas cylindrical micelles were observed with four stearic acids (**15**). (b) These cylindrical micelles were capable of encapsulating Nile Red, leading to the cellular uptake of Nile Red loaded Tat-functionalized cylindrical micelles by HeLa cells. Adapted from ref. 87 with permission from Wiley-VCH.

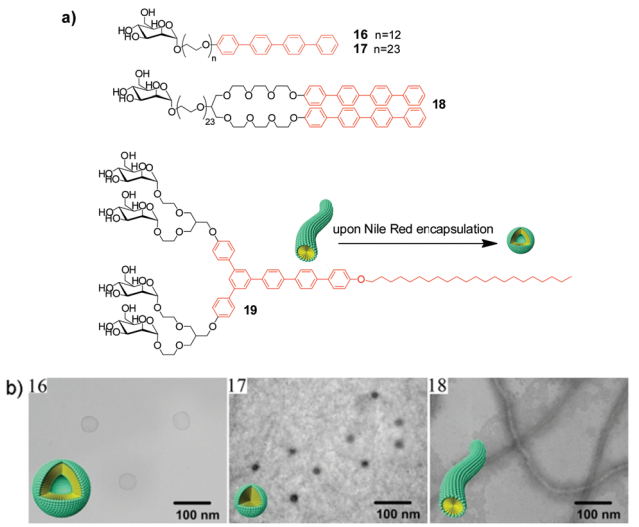

Fig. 10 Mannose-decorated aromatic rod-coil amphiphiles. Adapted from ref. 88 with permission from American Chemical Society.

rod-coil amphiphiles with a hydrophobic tetra(*p*-phenylene) segment (Fig. 10). Through systematic variation of the volume fraction between the hydrophobic and hydrophilic segments, different self-assembling morphologies ranging from vesicles (**16**) and spherical micelles (**17**) to cylindrical micelles (**18**) were achieved.[88] These systems functioned as very effective multivalent ligands for the lectin concanavalin A and *E. coli* bacteria. A 1800-fold increase in relative inhibitory potency compared with α-D-methyl mannose was observed for the spherical micellar architectures (**17**). The fact that the highest

binding affinity was obtained using a self-assembly with the highest curvature underlines the importance of the supramolecular architecture in the molecular recognition event.

The dendritic amphiphile **19** self-assembled into mannose coated cylindrical micelles with a length of about 200 nm (Fig. 10). Addition of the hydrophobic guest molecule Nile Red triggered the reversible transformation of these cylindrical micelles into spheres.[89] This self-assembling system thus responds to external signals and provides a rapid and reversible entry to different topologies. Binding studies with the lectin concanavalin A showed that both objects – cylindrical micelles and spheres – function as polyvalent inhibitors, but the motility of *E. coli* bacteria is more effectively inhibited with cylindrical micelles. The ability to systematically alter and control self-assembled structures in shape and size by molecular design can thus provide control over the biological activities of supramolecular materials. This is important since the strength and efficiency of polyvalent interactions are dependent on the shape and the surface properties of the interaction system.

In their recent work the group of Lee used the co-assembly of amphiphilic building blocks which differ in the crystallinity of their aromatic cores to control the length of self-assembled nanofibres.[90] Mixing the amphiphile **20**, which has a highly crystalline aromatic core, with amphiphile **21** disrupted the packing, leading to smaller fibres (Fig. 11b). *Via* co-assembly the length of the fibres could systematically be varied from a few micrometers to less than 70 nm. The ability of nanofibres of varying length to agglutinate bacteria was tested using agglutination index (AI) assays. The agglutination index systematically increased with the mole% of **20**, demonstrating that the length of the fibres has a significant influence on the formation of bacterial clusters (Fig. 11c). The increased bacterial agglutination with the increase in fibre length led to an increase in the inhibition of bacterial proliferation. This result shows that the differences in agglutination forces between fibres of varying length enable the fine-tuning of biological response.

A highly reproducible one-step method for generating (multi)functional fluorescent organic nanoparticles *via* self-assembly of pre-functionalized π-conjugated oligomers was reported by Schenning and co-workers.[40,91] The amphiphilic oligomers were on the one hand pre-functionalized with ligands for biological targeting, such as mannose (**24**), while on the other hand pre-functionalized with azides (**23**) to allow post-functionalization of pre-formed nanoparticles (Fig. 12a). The introduction of ligands at the extremities of inert ethylene glycol side-chains did not interfere with the self-assembly process. Additionally, mixing of the non-functionalized amphiphile **22** in different ratios with functionalized amphiphiles (**23**, **24**) prior to self-assembly in water enabled the reliable and reproducible tuning of ligand composition and density. *Via* copper catalyzed azide–alkyne cycloaddition (CuAAC) ligands could as well be successfully introduced at the nanoparticle surface after nanoparticle formation. The intrinsic fluorescence of these nanoparticles facilitated the evaluation of ligand densities and surface properties. Without the ligand, no unspecific adsorption was observed whereas the decoration with specific ligands induced selective binding of proteins, bacteria and magnetic beads to the nanoparticles (Fig. 12b and 12c). The comparison between pre- and post-functionalization revealed a significantly lower degree of ligand density *via* post-functionalization with alkyl mannose compared to the

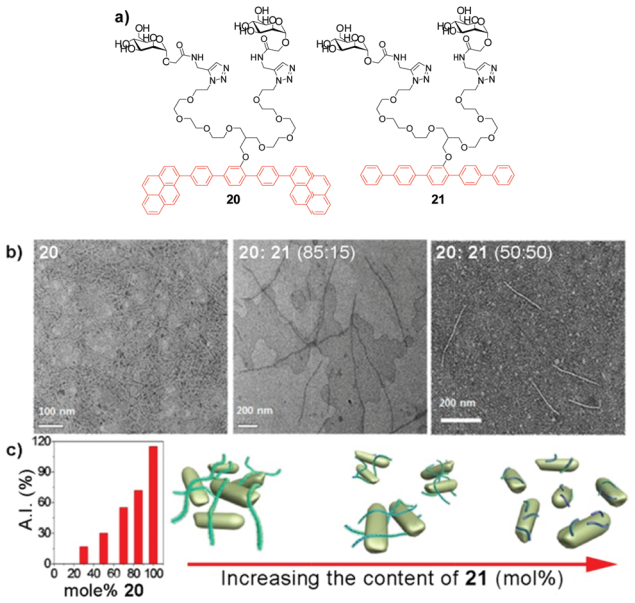

Fig. 11 (a) Mannose-decorated aromatic amphiphiles with differences in the crystallinity of the aromatic cores. (b) TEM micrographs of nanofibres formed by **20** and of small fibres formed upon co-assembly of **20** and **21** in different ratios. (c) Effect of the length of mannose-coated nanofibres on bacterial agglutination. The degree of agglutination is represented by the agglutination index (AI). Agglutination decreases with decreased fibre length. Adapted from ref. 90 with permission from American Chemical Society.

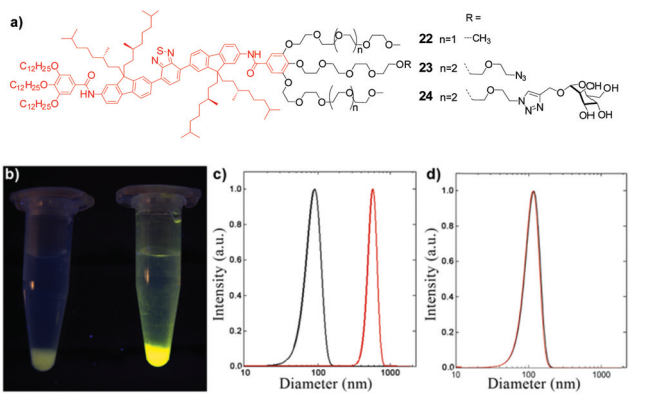

Fig. 12 Fluorescent π-conjugated self-assembling amphiphiles. (b) Photograph of washed *E. coli* bacteria under UV illumination after incubation with azide-nanoparticles (left, **22** : **23**; 1 : 1) and mannose-nanoparticles (right, **22** : **24**; 1 : 1). (c) Hydrodynamic diameter of mannose-nanoparticles before (black) and after the addition of the lectin ConA (red) measured by dynamic light scattering. (d) Hydrodynamic diameter of azide-nanoparticles before (black) and after the addition of the lectin ConA (red) measured by dynamic light scattering. Adapted from ref. 40 with permission from American Chemical Society.

ligand density achieved *via* self-assembly of mannose pre-functionalized amphiphile **24**. Combining both pre- and post-functionalization it was possible to generate multifunctional nanoparticles with the potential for multi-targeting, thus expanding the ligand diversity at two independent stages in the nanoparticle fabrication process.

3.4 Disc-shaped amphiphiles

In contrast to linear amphiphiles such as phospholipids and peptide amphiphiles, the self-assembly of C_3-symmetrical disc-shaped molecules leads to the selective formation of only one type of aggregate form: columnar stacks, due to their molecular geometry.

The discotic amphiphiles described by Besenius *et al.* consist of a C_3-symmetrical benzene-1,3,5-tricarboxamide core, a motif that self-assembles into triple hydrogen bonded helices. Extension of the core with (fluorinated) phenylalanine and aminobenzoate moieties stabilizes the assembly through additional π–π interactions, solvophobic effects and shielding of the core (Fig. 13).[92] The discotic scaffold itself self-assembles into columnar structures of 50–75 nm at millimolar concentrations, which increase in length with concentration. To yield supramolecular contrast agents for magnetic resonance imaging (MRI), different chelating ligands were introduced at the periphery.[93] The increasing ionic character of the introduced ligands led, through electrostatic repulsion, to the formation of small nearly spherical structures of around eleven monomers.[92] Functionalization with peptides as well led to changes in morphology and stability of the supramolecular polymers. Long and very stable rods were formed with a tendency to form bundles.[94] Dilution of peptide-functionalized discotics with Gd(III)–DOTA functionalized discotics prevented

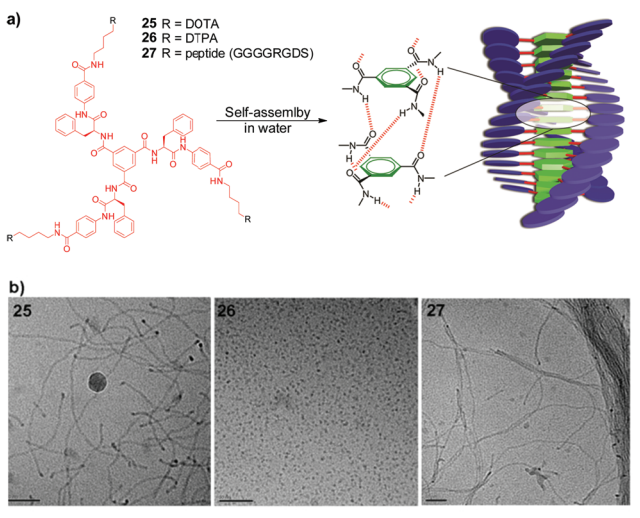

Fig. 13 (a) Phenylalanine containing discotic amphiphiles and their self-assembly in water. Adapted from ref. 92 with permission from National Academy of Sciences, U.S.A. (b) Cryo-TEM micrographs for self-assembled discotic amphiphiles (**25**, 0.66 mM; **26**, 1 mM; **27**, 1 mg mL^{-1}) vitrified at 288 K in citrate buffer (100 mM, pH 6); scale bar represents 50 nm. Adapted from ref. 92 with permission from National Academy of Sciences, U.S.A and from ref. 94 with permission from Royal Society of Chemistry.

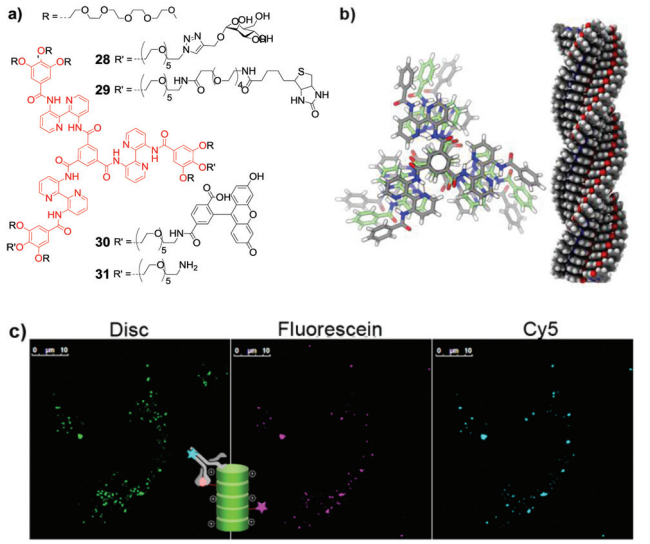

Fig. 14 (a) Bipyridine containing discotic amphiphiles. (b) The self-assembly of these amphiphiles in water. Adapted from ref. 98 with permission from Royal Society of Chemistry. (c) Confocal images of HeLa cells incubated for 1 h with a 5 μM mixture of **31**, **30** and **29** (80 : 10 : 10). To visualize the biotin functionalized discotic **29**, after 24 h the cells were fixed and stained with a Cy5-labelled anti-biotin antibody. Adapted from ref. 101 with permission from the American Chemical Society.

the peptide induced secondary interactions. These results again underline that the introduction of a ligand can significantly influence the self-assembly of a supramolecular scaffold. This at the same time allows for the fine-tuning of the length/shape of self-assembly through a balancing of attractive and repulsive forces.

Other studies have addressed discotics with an extended aromatic core of three 2,2′-bipyridine-3,3′-diamine molecules linked to a central benzene-1,3,5-tricarbonyl unit (Fig. 14a).[95,96] This inner core is surrounded by three gallic acid moieties functionalized with in total nine ethylene glycol chains which induce water-solubility and shield the hydrophobic core. The discotics are intrinsically fluorescent, which was used for evaluation of binding events using Förster resonance energy transfer (FRET) and to confirm the presence of self-assembling structures, as the fluorescent lifetime of the monomers increases upon self-assembly into columnar polymers.[97] The self-assembly of these discotics is based on strong intramolecular hydrogen bonding between the amide N–H groups and neighbouring bipyridine N-atoms, which preorganizes the molecules into an on average planar C_3-symmetrical conformation, allowing the molecules to form long stacks primarily through π–π stacking (Fig. 14b).[98] The introduction of functional groups at the periphery of the ethylene oxide tails enabled functionalization with bioactive ligands without interfering with the self-assembly.

Discotics bearing three azide functionalities were decorated with three mannose moieties (**28**) which led to selective binding to FimH receptor expressing *E. coli* bacteria.[99] The multivalent display of mannose ligands induced enhanced binding affinity through multivalency as quantified using an

enzyme-linked lectin assay. Functionalization of amine bearing discotics (**31**) with biotin (**29**) enabled the display of streptavidin – a biotin-binding protein – along the supramolecular polymer.[100] Förster resonance energy transfer (FRET) between differently labeled streptavidins indicated the approximation of those proteins along the supramolecular polymer. In both examples, the bare scaffold itself did not show any unspecific interactions with proteins and bacteria. In contrast to the bare and ligand functionalized discotics, the amine-functionalized discotics (**31**) showed cellular uptake at low μM concentrations; visualized by their auto-fluorescence using live cell multiphoton fluorescence microscopy.[101] Cellular uptake systems have since been developed based on these cell-permeable discotics. The dynamic intermixing of several supramolecular polymers generated supramolecular copolymers containing the cell-permeable discotic **31** along with up to two non-cell-permeable ligand functionalized discotics (**29**, **30**). These supramolecular copolymers were internalized by several cancer cell lines and co-localization of signals from all the co-assembled monomers was observed inside the cells (Fig. 14c). The amine functionalized discotics acted as carrier molecules, enabling the cellular uptake of the non-cell-permeable discotics by virtue of their combined presence in the supramolecular copolymer. The possibility to functionalize these discotics without interfering with the self-assembly combined with the ability to generate multi-component supramolecular polymers demonstrates the potential of the discotic scaffold as a versatile, flexibly decorated platform for several biological applications.

3.5 Host–guest complexation based self-assembly

The field of supramolecular chemistry started with the discovery of crown-ethers and their ability to complex ions in organic solvents. In aqueous solutions amphiphilic cavitands with a hydrophilic exterior and a hydrophobic interior, such as cyclodextrins or cucurbit[*n*]urils, are now widely used for the generation of biomaterials[33,102,103] and in fluorescence assays.[104] These hosts bind hydrophobic guest molecules to their interior with high binding affinities. Cyclodextrins are cyclic oligosaccharides consisting of six to eight D-glucopyranoside units linked by an α-1,4-glycosidic bond. Their ability to form complexes with larger hydrophobic guests has led to multiple applications in drug delivery as well as in the cosmetic and food industry.[105] Cucurbit[*n*]urils are cyclic cavitands based on the repeating monomer units of glycoluril. The displacement of a bound guest by a higher affinity guest (Fig. 15) introduces an element of switchability to host–guest based systems. The group of Scherman used cucurbit[8]uril and its ability to simultaneously bind two different guests as a ternary complex, to generate and assemble host–guest based amphiphiles into vesicles. After cellular uptake the disassembly of these vesicles could be triggered with a competing guest molecule, thus regulating the toxicity of this supramolecular system.[106]

3.5.1. Pseudopolyrotaxanes. The role of flexibility and adaptability in binding events is a key issue in the field of molecular recognition and has been studied using

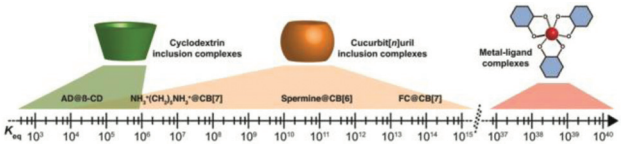

Fig. 15 Schematic representation of supramolecular binding motifs – cyclodextrin (left) and cucurbit[*n*]uril (middle) inclusion complexes together with catechol–iron complexes (right) – and the range of their typical equilibrium binding constants (AD = adamantane, FC = ferrocene). Reprinted from ref. 32 with permission from Royal Society of Chemistry.

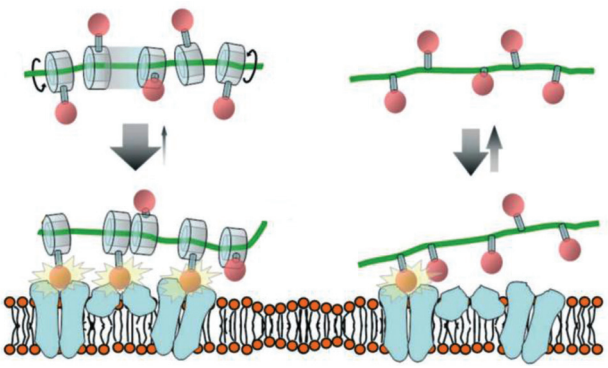

Fig. 16 Adjustment of ligand positioning of pseudopolyrotaxanes (left) and covalent polymers (right). Reprinted from ref. 109 with permission from Wiley-VCH.

pseudopolyrotaxenes. Polyrotaxanes are defined as a molecular assembly, in which several cyclic molecules are threaded onto a linear chain capped with sterically hindered 'bulky' end-groups.[107] In pseudopolyrotaxanes the linear chain is not capped with bulky end-groups. In contrast to previously discussed supramolecular assemblies, this supramolecular polymer does not possess a strongly defined topological shape. The non-covalently threaded cyclic molecules may rotate and slide along the polymeric chain facilitating the adjustment of ligand positioning to the encountered polyvalent target. This mobility should eliminate the spatial mismatching between ligands and receptors, which can occur at high ligand densities in covalently functionalized multivalent polymers (Fig. 16).[108]

The groups of Stoddart and Kim have studied pseudopolyrotaxanes as adaptable multivalent inhibitors. Both groups have used different cyclic molecules threaded by a polyviologen AB-copolymer, consisting of alternating decamethylene (A) and positively charged bipyridinium (B) segments. The group of Stoddard pioneered in the use of lactose functionalized α-CD,[110–112] while the group of Kim used mannose functionalized cucurbit[6]uril (CB[6]) (Fig. 17).[113] Stabilized by hydrophobic interactions at the interior of their cavities, both cyclic molecules predominantly rest on the decamethylene segments. The flanking charged bipyridinium segments act as electronic "speed bumps", reducing the translational movement. In the case of cucurbit[6]urils an additional charge–dipole interaction between the bipyridinium units and the CB[6]

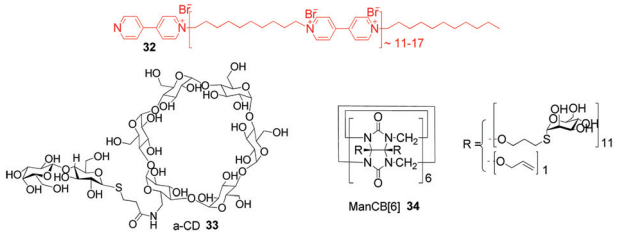

Fig. 17 Pseudopolyrotaxane building blocks.

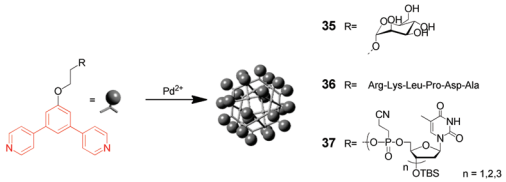

Fig. 18 Metal–ligand coordinated self-assembly. Adapted from ref. 119 with permission from American Chemical Society.

portal oxygen atoms stabilizes the assembly, and no appreciable dethreading is observed after a long period of time.[114] By contrast, cyclodextrins undergo measurable degrees of dethreading within hours of sample dilution, due to the lack of stabilizing charge–dipole interactions present in the case of CB[6].

The pseudopolyrotaxane from the group of Stoddart consists of a polyviologen-AB-copolymer with approximately 11–17 viologen units (**32**) fully threaded through mono-lactose functionalized α-cyclodextrins **33**. Their ability to inhibit the binding of galectin-1 to T-cells was assessed using the T-cell agglutination assay. The lactose binding sites in galectin-1 are located on opposite faces of the protein and long spacers between the carbohydrates are required to span the distance. Therefore, only small valency corrected inhibition enhancements were observed using dendritic systems.[110] This pseudopolyrotaxane, when compared with a lactose bearing polymer, showed a 6-fold valency corrected enhancement in a T-cell agglutination assay. Further, the influence of the length of the polyviologen chain and the degree of threading was investigated. A longer polyviologen chain, which can bridge longer distances, was observed to be more effective in the T-cell agglutination assay, while a lower degree of threading led to enhanced inhibitory properties.

In the pseudopolyrotaxane system of Kim *et al.*, cucurbit[6]uril was functionalized with on average eleven mannose moieties. Different amounts of these mannosylated CB[6]s (ManCB[6], **34**) were mixed with polyviologen, thus generating three mannose functionalized pseudopolyrotaxanes bearing 3, 5 or 10 ManCB[6] (Fig. 17). As control experiments, galactose and glucose functionalized pseudopolyrotaxanes were prepared. In both bacterial aggregation and hemagglutination assay the mannose pseudopolyrotaxane systems were much more effective than ManCB[6] alone. As well here, the pseudopolyrotaxane threaded through only three ManCB[6] was the most potent inhibitor, showing 300 times higher inhibitory potency than monomeric methyl-α-D-mannose, probably by providing the proper density of mannose. This pseudopolyrotaxane was capable of inhibiting the adhesion of ORN178 bacteria to urinary epithelial cells, a model for urinary tract infection. Upon decoration of cyclodextrins with positively charged groups the pseudopolyrotaxanes can as well be used for gene delivery.[115] Capping the rotaxane chain with folate, for example, was shown to increase the specificity of these transfection agents for tumor cells.[116]

3.6 Metal–ligand coordination

The group of Fujita obtained supramolecular polyvalent self-assemblies of a spherical type of topology using well-defined metal–ligand coordination. Here the formation of a well-defined metal–organic framework of 12 paladium(II) ions with 24 1,3-bis(4-pyridyl)phenyl groups is the main driving force of self-assembly. Incorporation of different bioactive ligands into this organic building block yielded spheres with precisely 24 hexapeptides,[117] DNA oligonucleotides[118] or carbohydrates[119] at the periphery (Fig. 18).

The spheres coated with different saccharides such as α-mannopyranoside, α-galactopyranoside, α- and β-glycopyranoside were used to study the formation of aggregates upon lectin binding. Concanavalin A, an α-mannopyranoside and α-glycopyranoside binding lectin, formed aggregates with only the α-mannopyranoside or α-glycopyranoside coated spheres. Addition of an excess of the corresponding carbohydrate reversed the formation of colloidal aggregates. Peanut agglutinin (PNA), a galactose-binding lectin, formed aggregates only with β-galactose coated spheres, indicating that the lectins recognize the terminal carbohydrate units of the spheres. This system shows high potential for the generation of spheres with encapsulated compounds, such as drugs, which can be released upon cell recognition by the bioactive ligand attached to this supramolecular platform. Metal–ligand coordination can as well be combined with host–guest complexation to generate highly complex multivalent assemblies as recently shown by Seeberger and co-workers, expanding the scope of possible structures, sizes and valencies.[120]

4. Conclusions

Supramolecular chemistry allows the rapid formation of nano-sized architectures. For self-assembly in water, amphiphilic molecules have emerged as versatile building blocks which can be synthetically programmed to self-assemble into a wide range of different topologies. The ability to decorate the generated nano-structures with bioactive epitopes has led to applications ranging from imaging to diagnostics, and from drug delivery to tissue engineering. The possibility to decorate the self-assembling systems prior- and post-assembly has additionally expanded the level of control over ligand composition, density, and diversity. The future success of bioactive self-assembling nanostructures in biomedical applications strongly depends on the ability to fine-tune the density and display of

bioactive epitopes – creating more complex heterovalent structures – while not interfering with the self-assembly process. Therefore, the development of bioactive self-assembling structures is strongly coupled to a detailed understanding of the self-assembling properties of the system; its dynamics, stability and its susceptibility to changes. This is highlighted by the fact that for the ligand decoration of many of the supramolecular systems described above less is almost certainly more; *e.g.* a lower ligand loading entails enhanced binding or inhibition of the biological target at hand.

While the design and understanding of the self-assembly of bare self-assembling scaffolds has advanced in recent years, the decoration with bioactive ligands often leads to unexpected changes in the self-assembly (see *e.g.*, Fig. 13). In particular, the introduction of ligands into highly crystalline assemblies, such as alpha-helical based self-assemblies, is frequently only marginally tolerated, since it leads to defects in the self-assembling structure. In contrast, the simultaneous introduction of several self-assembling elements, such as the combination of a beta-sheet peptide and a lipid tail in peptide amphiphiles, generates stable systems which can tolerate the introduction of different ligands. The unforeseen changes in the self-assembling structures upon ligand functionalization are, however, a beautiful new entry to expand the scope of sizes, stabilities and shapes of self-assembling systems. These changes at the same time provide more molecular insights into these fascinating bioactive supramolecular architectures.

Acknowledgements

Funded by ERC grants 204554 – SupraChemBio and 310275 – BioNLight and CTMM – 03O-201 Mammoth.

Notes and references

1 D. Philp and J. F. Stoddart, *Angew. Chem., Int. Ed.*, 1996, **35**, 1154–1196.
2 B. Alberts, *Molecular Biology of the Cell*, Taylor & Francis, 5th edn, 2007.
3 A. Ben-Shem, L. Jenner, G. Yusupova and M. Yusupov, *Science*, 2010, **330**, 1203–1209.
4 J. Taipale and J. Keski-Oja, *FASEB J.*, 1997, **11**, 51–59.
5 S. Miyamoto, S. K. Akiyama and K. M. Yamada, *Science*, 1995, **267**, 883–885.
6 R. N. Germain, *Curr. Biol.*, 1997, **7**, R640–R644.
7 R. F. A. Zwaal, P. Comfurius and E. M. Bevers, *Cell. Mol. Life Sci.*, 2005, **62**, 971–988.
8 B. Garnier, A. Bouter, C. Gounou, K. G. Petry and A. R. Brisson, *Bioconjugate Chem.*, 2009, **20**, 2114–2122.
9 M. A. Wear, D. A. Schafer and J. A. Cooper, *Curr. Biol.*, 2000, **10**, R891–R895.
10 J. Avila, *FASEB J.*, 1990, **4**, 3284–3290.
11 M. Mammen, S. Choi and G. M. Whitesides, *Angew. Chem., Int. Ed.*, 1998, **37**, 2754–2794.
12 C. Fasting, C. A. Schalley, M. Weber, O. Seitz, S. Hecht, B. Koksch, J. Dernedde, C. Graf, E.-W. Knapp and R. Haag, *Angew. Chem., Int. Ed.*, 2012, **51**, 10472–10498.
13 J. Lehn, *Science*, 1993, **260**, 1762–1763.
14 J.-M. Lehn, *Science*, 2002, **295**, 2400–2403.
15 C. J. Pedersen, *J. Am. Chem. Soc.*, 1967, **89**, 7017–7036.
16 A. Ciferri, *Supramolecular Polymers*, Taylor & Francis, 2nd edn, 2005.
17 G. V. Oshovsky, D. N. Reinhoudt and W. Verboom, *Angew. Chem., Int. Ed.*, 2007, **46**, 2366–2393.
18 J.-H. Ryu, D.-J. Hong and M. Lee, *Chem. Commun.*, 2008, 1043–1054.
19 Y. Gao, J. Shi, D. Yuan and B. Xu, *Nat. Commun.*, 2012, **3**, 1033.
20 D. Ye, G. Liang, M. L. Ma and J. Rao, *Angew. Chem., Int. Ed.*, 2011, **50**, 2275–2279.
21 D. A. Uhlenheuer, K. Petkau and L. Brunsveld, *Chem. Soc. Rev.*, 2010, **39**, 2817–2826.
22 R. A. Lerner, *Angew. Chem., Int. Ed.*, 2006, **45**, 8106–8125.
23 V. P. Torchilin, *Adv. Drug Delivery Rev.*, 2006, **58**, 1532–1555.
24 J. Hrkach, D. V. Hoff, M. M. Ali, E. Andrianova, J. Auer, T. Campbell, D. D. Witt, M. Figa, M. Figueiredo, A. Horhota, S. Low, K. McDonnell, E. Peeke, B. Retnarajan, A. Sabnis, E. Schnipper, J. J. Song, Y. H. Song, J. Summa, D. Tompsett, G. Troiano, T. V. G. Hoven, J. Wright, P. LoRusso, P. W. Kantoff, N. H. Bander, C. Sweeney, O. C. Farokhzad, R. Langer and S. Zale, *Sci. Transl. Med.*, 2012, **4**, 128ra39.
25 N. Stephanopoulos, G. J. Tong, S. C. Hsiao and M. B. Francis, *ACS Nano*, 2010, **4**, 6014–6020.
26 D. E. Discher and F. Ahmed, *Annu. Rev. Biomed. Eng.*, 2006, **8**, 323–341.
27 A. Louie, *Chem. Rev.*, 2010, **110**, 3146–3195.
28 P. Y. W. Dankers and E. W. Meijer, *Bull. Chem. Soc. Jpn.*, 2007, **80**, 2047–2073.
29 J. H. Collier, *Soft Matter*, 2008, **4**, 2310–2315.
30 F. Zhao, M. L. Ma and B. Xu, *Chem. Soc. Rev.*, 2009, **38**, 883–891.
31 P. Y. W. Dankers, M. C. Harmsen, L. A. Brouwer, M. J. A. V. Luyn and E. W. Meijer, *Nat. Mater.*, 2005, **4**, 568–574.
32 E. A. Appel, J. del Barrio, X. J. Loh and O. A. Scherman, *Chem. Soc. Rev.*, 2012, **41**, 6195.
33 E. A. Appel, X. J. Loh, S. T. Jones, F. Biedermann, C. A. Dreiss and O. A. Scherman, *J. Am. Chem. Soc.*, 2012, **134**, 11767–11773.
34 J. H. Collier, J. S. Rudra, J. Z. Gasiorowski and J. P. Jung, *Chem. Soc. Rev.*, 2010, **39**, 3413–3424.
35 J. B. Matson and S. I. Stupp, *Chem. Commun.*, 2012, **48**, 26–33.
36 J. Z. Gasiorowski and J. H. Collier, *Biomacromolecules*, 2011, **12**, 3549–3558.
37 G. A. Silva, C. Czeisler, K. L. Niece, E. Beniash, D. A. Harrington, J. A. Kessler and S. I. Stupp, *Science*, 2004, **303**, 1352–1355.

38 A. Barnard and D. K. Smith, *Angew. Chem., Int. Ed.*, 2012, **51**, 6572–6581.
39 F. Gu, L. Zhang, B. A. Teply, N. Mann, A. Wang, A. F. Radovic-Moreno, R. Langer and O. C. Farokhzad, *Proc. Natl. Acad. Sci. U. S. A.*, 2008, **105**, 2586–2591.
40 K. Petkau, A. Kaeser, I. Fischer, L. Brunsveld and A. P. H. J. Schenning, *J. Am. Chem. Soc.*, 2011, **133**, 17063–17071.
41 D. J. Toft, T. J. Moyer, S. M. Standley, Y. Ruff, A. Ugolkov, S. I. Stupp and V. L. Cryns, *ACS Nano*, 2012, **6**, 7956–7965.
42 D. N. Woolfson and Z. N. Mahmoud, *Chem. Soc. Rev.*, 2010, **39**, 3464–3479.
43 W. R. Algar, D. E. Prasuhn, M. H. Stewart, T. L. Jennings, J. B. Blanco-Canosa, P. E. Dawson and I. L. Medintz, *Bioconjugate Chem.*, 2011, **22**, 825–858.
44 T. Perrier, P. Saulnier and J. Benoît, *Chem.–Eur. J.*, 2010, **16**, 11516–11529.
45 E. Lallana, A. Sousa-Herves, F. Fernandez-Trillo, R. Riguera and E. Fernandez-Megia, *Pharm. Res.*, 2012, **29**, 1–34.
46 L. A. Canalle, D. W. P. M. Löwik and J. C. M. van Hest, *Chem. Soc. Rev.*, 2010, **39**, 329–353.
47 S. F. M. van Dongen, H.-P. M. de Hoog, R. J. R. W. Peters, M. Nallani, R. J. M. Nolte and J. C. M. van Hest, *Chem. Rev.*, 2009, **109**, 6212–6274.
48 D. W. Pack, A. S. Hoffman, S. Pun and P. S. Stayton, *Nat. Rev. Drug Discovery*, 2005, **4**, 581–593.
49 N. F. Steinmetz, *Nanomed. Nanotechnol.*, 2010, **6**, 634–641.
50 J. I. Cutler, E. Auyeung and C. A. Mirkin, *J. Am. Chem. Soc.*, 2012, **134**, 1376–1391.
51 Themed issue on Nanomedicine, *Chem. Soc. Rev.*, 2012, **41**, 2521–3012.
52 A. Dominguez, A. Fernandez, N. Gonzalez, E. Iglesias and L. Montenegro, *J. Chem. Educ.*, 1997, **74**, 1227–1231.
53 H. Ringsdorf, B. Schlarb and J. Venzmer, *Angew. Chem., Int. Ed. Engl.*, 1988, **27**, 113–158.
54 A. D. Bangham, *BioEssays*, 1995, **17**, 1081–1088.
55 W. T. Al-Jamal and K. Kostarelos, *Acc. Chem. Res.*, 2011, **44**, 1094–1104.
56 W. J. M. Mulder, G. J. Strijkers, G. A. F. van Tilborg, D. P. Cormode, Z. A. Fayad and K. Nicolay, *Acc. Chem. Res.*, 2009, **42**, 904–914.
57 E. Forssen and M. Willis, *Adv. Drug Deliverery Rev.*, 1998, **29**, 249–271.
58 A. L. Klibanov, K. Maruyama, V. P. Torchilin and L. Huang, *FEBS Lett.*, 1990, **268**, 235–237.
59 E. Kluza, D. W. J. van der Schaft, P. A. I. Hautvast, W. J. M. Mulder, K. H. Mayo, A. W. Griffioen, G. J. Strijkers and K. Nicolay, *Nano Lett.*, 2010, **10**, 52–58.
60 Peptide- and protein-based materials themed issue, *Chem. Soc. Rev.*, 2010, **39**, 3337–3580.
61 A. L. Boyle and D. N. Woolfson, in *Supramolecular Chemistry: From Molecules to Nanomaterials*, John Wiley & Sons, Ltd, 2012, pp. 1639–1664.
62 A. Aggeli, M. Bell, L. M. Carrick, C. W. G. Fishwick, R. Harding, P. J. Mawer, S. E. Radford, A. E. Strong and N. Boden, *J. Am. Chem. Soc.*, 2003, **125**, 9619–9628.
63 L. C. Serpell, *Biochim. Biophys. Acta, Mol. Basis Dis.*, 2000, **1502**, 16–30.
64 Y. Takahashi, A. Ueno and H. Mihara, *ChemBioChem*, 2002, **3**, 637–642.
65 U. Baxa, V. Speransky, A. C. Steven and R. B. Wickner, *Proc. Natl. Acad. Sci. U. S. A.*, 2002, **99**, 5253–5260.
66 A. J. Baldwin, R. Bader, J. Christodoulou, C. E. MacPhee, C. M. Dobson and P. D. Barker, *J. Am. Chem. Soc.*, 2006, **128**, 2162–2163.
67 Y. Lim, E. Lee and M. Lee, *Angew. Chem., Int. Ed.*, 2007, **46**, 3475–3478.
68 S. L. Gras, A. K. Tickler, A. M. Squires, G. L. Devlin, M. A. Horton, C. M. Dobson and C. E. MacPhee, *Biomaterials*, 2008, **29**, 1553–1562.
69 J. S. Rudra, Y. F. Tian, J. P. Jung and J. H. Collier, *Proc. Natl. Acad. Sci. U. S. A.*, 2010, **107**, 622–627.
70 H. Kodama, S. Matsumura, T. Yamashita and H. Mihara, *Chem. Commun.*, 2004, 2876–2877.
71 Y. Lim, S. Park, E. Lee, H. Jeong, J.-H. Ryu, M. S. Lee and M. Lee, *Biomacromolecules*, 2007, **8**, 1404–1408.
72 Y. Lim, S. Park, E. Lee, J.-H. Ryu, Y.-R. Yoon, T.-H. Kim and M. Lee, *Chem. Asian J.*, 2007, **2**, 1363–1369.
73 K. Channon and C. E. MacPhee, *Soft Matter*, 2008, **4**, 647–652.
74 A. N. Lupas and M. Gruber, in *Fibrous Proteins: Coiled-Coils, Collagen and Elastomers*, Elsevier, Amsterdam, 2005, vol. 70, pp. 37–38.
75 M. G. Ryadnov, D. Papapostolou and D. N. Woolfson, in *Nanostructure Design*, Humana Press, 2008, vol. 474, pp. 35–51.
76 M. G. Ryadnov, A. Bella, S. Timson and D. N. Woolfson, *J. Am. Chem. Soc.*, 2009, **131**, 13240–13241.
77 Z. N. Mahmoud, S. B. Gunnoo, A. R. Thomson, J. M. Fletcher and D. N. Woolfson, *Biomaterials*, 2011, **32**, 3712–3720.
78 M. G. Ryadnov and D. N. Woolfson, *J. Am. Chem. Soc.*, 2004, **126**, 7454–7455.
79 D. Papapostolou, E. H. C. Bromley, C. Bano and D. N. Woolfson, *J. Am. Chem. Soc.*, 2008, **130**, 5124–5130.
80 V. Villard, O. Kalyuzhniy, O. Riccio, S. Potekhin, T. N. Melnik, A. V. Kajava, C. Rüegg and G. Corradin, *J. Pept. Sci.*, 2006, **12**, 206–212.
81 J. D. Hartgerink, E. Beniash and S. I. Stupp, *Science*, 2001, **294**, 1684–1688.
82 J. D. Hartgerink, E. Beniash and S. I. Stupp, *Proc. Natl. Acad. Sci. U. S. A.*, 2002, **99**, 5133–5138.
83 V. M. Tysseling-Mattiace, V. Sahni, K. L. Niece, D. Birch, C. Czeisler, M. G. Fehlings, S. I. Stupp and J. A. Kessler, *J. Neurosci.*, 2008, **28**, 3814–3823.
84 H. Storrie, M. O. Guler, S. N. Abu-Amara, T. Volberg, M. Rao, B. Geiger and S. I. Stupp, *Biomaterials*, 2007, **28**, 4608–4618.
85 M. J. Webber, J. A. Kessler and S. I. Stupp, *J. Intern. Med.*, 2010, **267**, 71–88.
86 H. Cui, M. J. Webber and S. I. Stupp, *Biopolymers*, 2010, **94**, 1–18.

87 Y. Lim, E. Lee and M. Lee, *Angew. Chem., Int. Ed.*, 2007, **46**, 9011–9014.
88 B.-S. Kim, D.-J. Hong, J. Bae and M. Lee, *J. Am. Chem. Soc.*, 2005, **127**, 16333–16337.
89 J.-H. Ryu, E. Lee, Y. Lim and M. Lee, *J. Am. Chem. Soc.*, 2007, **129**, 4808–4814.
90 D.-W. Lee, T. Kim, I.-S. Park, Z. Huang and M. Lee, *J. Am. Chem. Soc.*, 2012, **134**, 14722–14725.
91 R. Abbel, R. van der Weegen, E. W. Meijer and A. P. H. J. Schenning, *Chem. Commun.*, 2009, 1697–1699.
92 P. Besenius, G. Portale, P. H. H. Bomans, H. M. Janssen, A. R. A. Palmans and E. W. Meijer, *Proc. Natl. Acad. Sci. U. S. A.*, 2010, **107**, 17888–17893.
93 P. Besenius, J. L. M. Heynens, R. Straathof, M. M. L. Nieuwenhuizen, P. H. H. Bomans, E. Terreno, S. Aime, G. J. Strijkers, K. Nicolay and E. W. Meijer, *Contrast Media Mol. Imaging*, 2012, **7**, 356–361.
94 P. Besenius, Y. Goedegebure, M. Driesse, M. Koay, P. H. H. Bomans, A. R. A. Palmans, P. Y. W. Dankers and E. W. Meijer, *Soft Matter*, 2011, **7**, 7980–7983.
95 A. R. A. Palmans, J. A. J. M. Vekemans, H. Fischer, R. A. Hikmet and E. W. Meijer, *Chem.–Eur. J.*, 1997, **3**, 300–307.
96 L. Brunsveld, B. G. G. Lohmeijer, J. A. J. M. Vekemans and E. W. Meijer, *Chem. Commun.*, 2000, 2305–2306.
97 L. Brunsveld, H. Zhang, M. Glasbeek, J. A. J. M. Vekemans and E. W. Meijer, *J. Am. Chem. Soc.*, 2000, **122**, 6175–6182.
98 T. Metzroth, A. Hoffmann, R. Martin-Rapun, M. M. J. Smulders, K. Pieterse, A. R. A. Palmans, J. A. J. M. Vekemans, E. W. Meijer, H. W. Spiess and J. Gauss, *Chem. Sci.*, 2011, **2**, 69–76.
99 M. K. Müller and L. Brunsveld, *Angew. Chem., Int. Ed.*, 2009, **48**, 2921–2924.
100 M. K. Müller, K. Petkau and L. Brunsveld, *Chem. Commun.*, 2010, **47**, 310–312.
101 K. Petkau-Milroy, M. H. Sonntag, A. H. A. M. van Onzen and L. Brunsveld, *J. Am. Chem. Soc.*, 2012, **134**, 8086–8089.
102 A. Harada, Y. Takashima and H. Yamaguchi, *Chem. Soc. Rev.*, 2009, **38**, 875–882.
103 H. D. Nguyen, D. T. Dang, J. L. J. van Dongen and L. Brunsveld, *Angew. Chem., Int. Ed.*, 2010, **49**, 895–898.
104 R. N. Dsouza, A. Hennig and W. M. Nau, *Chem.–Eur. J.*, 2012, **18**, 3444–3459.
105 E. Bilensoy, *Cyclodextrins in Pharmaceutics, Cosmetics, and Biomedicine: Current and Future Industrial Applications*, John Wiley & Sons, 2011.
106 D. Jiao, J. Geng, X. J. Loh, D. Das, T.-C. Lee and O. A. Scherman, *Angew. Chem., Int. Ed.*, 2012, **51**, 9633–9637.
107 H. Hyun and N. Yui, *Macromol. Biosci.*, 2011, **11**, 765–771.
108 T. Hasegawa, S. Kondoh, K. Matsuura and K. Kobayashi, *Macromolecules*, 1999, **32**, 6595–6603.
109 N. Yui and T. Ooya, *Chem.–Eur. J.*, 2006, **12**, 6730–6737.
110 A. Nelson, J. M. Belitsky, S. Vidal, C. S. Joiner, L. G. Baum and J. F. Stoddart, *J. Am. Chem. Soc.*, 2004, **126**, 11914–11922.
111 J. M. Belitsky, A. Nelson, J. D. Hernandez, L. G. Baum and J. F. Stoddart, *Chem. Biol.*, 2007, **14**, 1140–1151.
112 J. M. Belitsky, A. Nelson and J. F. Stoddart, *Org. Biomol. Chem.*, 2006, **4**, 250–256.
113 J. Kim, Y. Ahn, K. M. Park, D.-W. Lee and K. Kim, *Chem.–Eur. J.*, 2010, **16**, 12168–12173.
114 S. Choi, J. W. Lee, Y. H. Ko and K. Kim, *Macromolecules*, 2002, **35**, 3526–3531.
115 T. Albuzat, M. Keil, J. Ellis, C. Alexander and G. Wenz, *J. Mater. Chem.*, 2012, **22**, 8558–8565.
116 Y. Zhou, H. Wang, C. Wang, Y. Li, W. Lu, S. Chen, J. Luo, Y. Jiang and J. Chen, *Mol. Pharm.*, 2012, **9**, 1067–1076.
117 M. Ikemi, T. Kikuchi, S. Matsumura, K. Shiba, S. Sato and M. Fujita, *Chem. Sci.*, 2010, **1**, 68–71.
118 T. Kikuchi, S. Sato and M. Fujita, *J. Am. Chem. Soc.*, 2010, **132**, 15930–15932.
119 N. Kamiya, M. Tominaga, S. Sato and M. Fujita, *J. Am. Chem. Soc.*, 2007, **129**, 3816–3817.
120 D. Grünstein, M. Maglinao, R. Kikkeri, M. Collot, K. Barylyuk, B. Lepenies, F. Kamena, R. Zenobi and P. H. Seeberger, *J. Am. Chem. Soc.*, 2011, **133**, 13957–13966.

